International Journal of Biometeorology
https://doi.org/10.1007/s00484-021-02162-5

ORIGINAL PAPER

A process-based model to simulate sugarcane orange rust severity from weather data in Southern Brazil

Taynara Tuany Borges Valeriano[1] · **Glauco de Souza Rolim**[2] · **Luisa Maria Manici**[1] · **Laura Giustarini**[3] · **Simone Bregaglio**[1]

Received: 17 July 2020 / Revised: 31 May 2021 / Accepted: 5 June 2021

Abstract

Forecasting the severity of plant diseases is an emerging need for farmers and companies to optimize management actions and to predict crop yields. Process-based models are viable tools for this purpose, thanks to their capability to reproduce pathogen epidemiological processes as a function of the variability of agro-environmental conditions. We formalized the key phases of the life cycle of *Puccinia kuenhii* (W. Krüger) EJ Butler, the causal agent of orange rust on sugarcane, into a new simulation model, called ARISE (Orange Rust Intensity Index). ARISE is composed of generic models of epidemiological processes modulated by partial components of host resistance and was parameterized according to *P. kuenhii* hydro-thermal requirements. After calibration and evaluation with field data, ARISE was executed on sugarcane areas in Brazil, India and Australia to assess the pathogen suitability in different environments. ARISE performed well in calibration and evaluation, where it accurately matched observations of orange rust severity. It also reproduced a large spatial and temporal variability in simulated areas, confirming that the pathogen suitability is strictly dependent on warm temperatures and high relative air humidity. Further improvements will entail coupling ARISE with a sugarcane growth model to assess yield losses, while further testing the model with field data, using input weather data at a finer resolution to develop a decision support system for sugarcane growers.

Keywords *Puccinia kuehnii* · Disease modeling · Process-based model · Severity index · Disease forecasting

Introduction

Orange rust caused by the polycyclic fungus *Puccinia kuehnii* (W. Krüger) EJ Butler is a relatively new emerging disease of sugarcane (Sentelhas et al. 2016; Chapola et al. 2016; Lima et al. 2017). A severe epidemic occurred in 1999–2000 in Australia, where yield losses reached up to 50%, causing an economic loss of 200 million Australian dollars (Magarey et al. 2001). Firstly, reported by Krüger in 1890 on sugarcane in the Java Island, the pathogen arrived in the western hemisphere as a consequence of global trade (Rott et al. 2016). In 2009, it was detected in Brazil in the São Paulo state (Barbasso et al. 2010) from where it spread in the main sugarcane areas (Chaves et al. 2013). Nowadays, orange rust disease is the most emerging threat to sugarcane yield in Brazil, which is the top producing and exporting country (Bordonal et al. 2018) with an annual production of 635 million tons of sugarcane (CONAB 2019).

Puccinia kuehnii is a *Basidiomycete*, from the *Uredinales* order and *Pucciniaceae* family (Hawksworth et al. 1995). The symptomatology caused by the pathogen on sugarcane plants manifests as pustules, which are uredinial lesions developing on the underside of the leaf, in oval shape and cinnamon to orange color (Magarey 2000). The damage associated with orange rust symptoms involves the reduction of the photosynthetic rates, of the stomatal conductance and of the transpiration efficiency of sugarcane crops (Zhao et al. 2011). The

The research of this paper was partly carried out while Taynara Tuany Borges Valeriano was at the School of Agricultural and Veterinarian Sciences, São Paulo State University (Unesp), Jaboticabal, Brazil.

✉ Taynara Tuany Borges Valeriano
taynara.valeriano@crea.gov.it

[1] CREA—Council for Agricultural Research and Economics, Research Centre for Agriculture and Environment, I-40128 Bologna, Italy

[2] School of Agricultural and Veterinarian Sciences, São Paulo State University (Unesp), Jaboticabal, Brazil

[3] Hazelnut Company Division, Ferrero Trading Luxembourg, Rue de Trèves, L, 2632 Findel, Luxembourg

Published online: 19 June 2021

epidemiology of orange rust largely depends on environmental conditions, with high moisture and warm temperatures favoring the increase of disease severity (Magarey 2000; Minchio et al. 2017).

Optimum temperature for infection range between 22 and 24 °C, with high air relative humidity prolonging leaf wetness duration favoring the epidemic development (Magarey et al. 2004). The leaves are asymptomatic up to the end of the latency period, which can range from 10 to 21 days depending on air temperature (Moreira et al. 2018). After this stage, pustules produce urediniospores, which are released into the air and are dispersed by wind. The optimal temperature range for sporulation is 19–26 °C, with high relative humidity favoring the process and wind speed playing a major role in spores' dispersal (Ferrari et al. 2013). The orange rust pathogen may present fully open pustules within 21 days after inoculation in some varieties (Mistura 2016) and has a significant evolutionary potential. It is able to fulfill a high number of cycles per growing season, and it can rapidly overcome host resistance, as demonstrated by laboratory studies carried out on pathogenic variants in Florida (Sanjel et al. 2016).

According to Araújo et al. (2013), yield losses caused by orange rust can exceed 40% on susceptible and moderately resistant varieties. Sugarcane growers contrast the disease by planting resistant varieties: nevertheless, several resistance breakdowns have occurred in recent years, and studies concerning the inheritance of resistance to orange rust of sugarcane in Brazil have been recently released (Klosowski et al. 2013a; Chapola et al. 2016). Nowadays, three to four fungicide applications year^{-1} are required in Florida to contain yield losses below the economic threshold (Rott et al. 2016). Reliable forecasting models of orange rust infection risk to optimize the timing and effectiveness of fungicide applications would be crucial to support in-season disease management. Simulation models have indeed the capability to extrapolate experimental results from one site to another (Basso et al. 2013), thus enabling the generation of alerts to optimize chemical control of plant diseases (Gillespie and Sentelhas 2008).

The first research applications towards releasing operational early warning systems of orange rust epidemics have been carried out in Florida (Chaulagain et al. 2020) and in Brazil (Sentelhas et al. 2016). The availability of process-based models to predict the variability of orange rust severity as a function of varietal susceptibility and weather conditions is the key building block of these forecasting systems. Additionally, the same models could also be used for the identification of adaptation strategies to climatic changes in the short and medium term (Manici et al. 2014).

We propose here a new process-based simulation model (ARISE, Orange Rust Intensity Index) of orange rust severity, composed by generic sub-models of the main phases of the epidemiological cycle, considering the effect of partial resistant components to infection, sporulation and latency. After evaluating model performances in reproducing field observations collected in Brazil, we applied ARISE over large areas in key sugarcane producing countries, where we analyzed its behavior and the variability of disease severity across environments.

Materials and methods

Developing the ARISE (Orange Rust Intensity Index) model

ARISE dynamically simulates main processes of the epidemiological cycle of *P. kuehnii* to provide an indicator of sugarcane orange rust severity, considering the impact of host resistance in reducing the disease severity. The model workflow comprises generic sub-models reproducing the process of infection, spore dispersal, latency duration and sporulation efficiency, which were parameterized according to the pathogen's thermal and moisture requirements (Fig. 1). Most sub-models implemented in ARISE adopt an hourly time step. The model is initialized on the first day of winter, when the suitability of weather conditions for the infection process begins to be simulated, together with the efficiency of spore dispersal as driven by daily wind speed. ARISE considers that a fulfilled infection event passes through the latency period, whose duration varies according to air temperature. When the latency period is accomplished, the efficiency of sporulation is simulated as a function of relative humidity and temperature and concurs to compute the ARISE severity. The ARISE model is driven by 17 parameters related to the epidemiological cycle of *P. kuehnii* (Table 1).

The simulation of the infection process of *P. kuhenii* is based on the suitability of thermal and moisture conditions in the form of leaf wetness duration. The dynamic version of the generic model (Bregaglio et al. 2012) for airborne fungal pathogens developed by Magarey et al. (2005) was parameterized according to literature data and used in ARISE. This model computes the air temperature response function Eq. 1 and produces a unitless output ranging from 0 to 1 (Yan and Hunt 1999), scaling it to the pathogen specific wetness duration requirement, according to Eq. 2.

$$f(T) = \left(\frac{Tmax - T}{Tmax - Topt}\right)\left(\frac{T - Tmin}{Topt - Tmin}\right)^{\left(\frac{Topt - Tmin}{Tmax - Topt}\right)} \quad (1)$$

$$\mathrm{f}(LW) = \begin{cases} \frac{LWmin}{f(T)} & if \quad \frac{LWmin}{f(T)} \leq LWmax \\ 0 & elsewhere \end{cases} \quad (2)$$

where f(LW) is the hourly leaf wetness response function, LWmin (hour) is the minimum leaf wetness duration for infection and LWmax (h) is the optimal leaf wetness duration

Table 1 Acronym, description, unit and literature source of the values of the parameters needed to reproduce the epidemiological cycle of *Puccinia kuehnii* in the ARISE model-based index

Parameter	Description	Unit	Reference[a]
TmaxInf	Maximum temperature for infection	°C	1, 2, 3, 4, 5, 6, 8
ToptInf	Optimum temperature for infection	°C	1, 2, 3, 4, 5, 6, 7, 8
TminInf	Minimum temperature for infection	°C	1, 2, 3, 4, 5, 6, 8
LWmax	Not limiting leaf wetness duration for infection	h	NA
LWmin	Minimum leaf wetness for infection	h	5, 6, 8
D50	Dry hours to stop an infection event	h	NA
WSmax	Maximum wind speed for dispersal	m s^{-1}	9, 10
WS50	Wind speed for dispersal 50% of spores	m s^{-1}	NA
WSmin	Minimum wind speed for dispersal	m s^{-1}	9, 10
TmaxL	Maximum temperature for latency	°C	1, 2, 3, 4, 5, 6, 8
ToptL	Optimum temperature for latency	°C	1, 2, 3, 4, 5, 6, 7, 8
TminL	Minimum temperature for latency	°C	1, 2, 3, 4, 5, 6, 8
LDmin	Minimum latency duration	days	8, 11
TmaxS	Maximum temperature for sporulation	°C	12
ToptS	Optimum temperature for sporulation	°C	12
TminS	Minimum temperature for sporulation	°C	12
RHminS	Minimum relative humidity for sporulation	%	1, 7

[a] 1: Infante et al. (2009); 2: Hsieh et al. (1977); 3: Minchio et al. (2011); 4: Minchio et al. (2017); 5: Vaseduva (1958); 6: Lima et al. (2017); 7: Magarey et al. (2004); 8: Martins (2010); 9: Ferrari et al. (2013); 10: Mallaiah and Rao (1982); 11: Moreira et al. (2018); 12: Hsieh and Fang (1981)

for the completion of an infection event. T (°C) is hourly air temperature, Tmin, Tmax and Topt (°C) are pathogen specific cardinal temperatures for infection. The model considers the impact of a dry period on the infection process by means of a

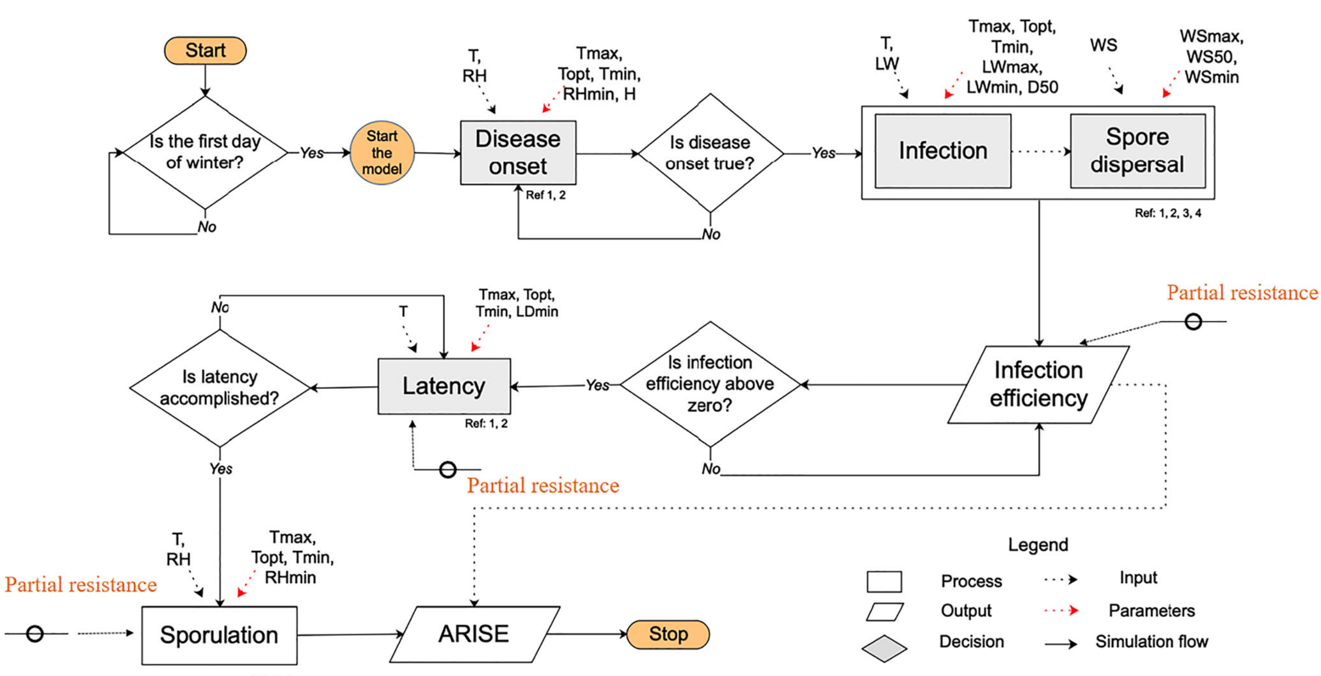

Fig. 1 Conceptual diagram of the processes simulated by the ARISE model. T (°C), air temperature; Tmax (°C), maximum temperature; Topt (°C) optimal temperature; Tmin (°C), minimum temperature; RH (%), relative humidity; RHmin (%), minimum relative humidity; H (h), threshold; LW (true/false), leaf wetness; LWmax (h), maximum leaf wetness; LWmin (h), minimum leaf wetness; D50 (h), dry hours to stop an infection event; WS (m s^{-1}), wind speed; WSmax (m s^{-1}), maximum wind speed; WSmin (m s^{-1}), minimum wind speed; WS50 (m s^{-1}), wind speed for dispersion of 50% of the spores; LDmin (h), latency duration minimum; ARISE (unitless), Orange Rust Intensity Index. [1]Bregaglio and Donatelli (2015); [2]Yan and Hunt (1999); [3]Magarey et al. (2005); [4]Aylor (1982)

critical interruption value (D50, h), as reported in Eq. 3 (Bregaglio and Donatelli 2015):

$$Wsum = \begin{cases} W_1 + W_2 & D < D50 \\ W_1, W_2 & elsewhere \end{cases} \quad (3)$$

where Wsum (h) is the cumulated duration of a leaf wetness period and W1 and W2 (h) are two wet periods separated by an interruption, D(h). The model considers two wet periods as separated when D ≥ D50. An infection event is fulfilled when Wsum > f(T); when Wsum < f(W), the infection event remains incomplete and is evaluated in the following hour.

ARISE then computes the efficiency of spore dispersal on a daily time step according to Aylor (1982), as a function of average daily wind speed (Eqs. 4–7):

$$f(SP) = \begin{cases} 0 & if\ WS < WSmin \\ \dfrac{(WS-WSmin)^2}{(WS-WSmin)^2 + (Ws50-WSmin)^2} & if\ WSmin \le WS \le WS50 \\ \dfrac{(WS-WSmin)^2}{(WS-WSmin)^2 + (WS50-WSmin)^2 c} & if\ WS50 < WS \le WSmax \\ 1 & if\ WS > WSmax \end{cases} \quad (4)$$

$$c = b + aWS \quad (5)$$

$$b = 1 - aWS50 \quad (6)$$

$$a = \frac{1}{WSmax - WS50} \quad (7)$$

where WS (m s^{-1}) is the daily wind speed, WSmin (m s^{-1}) is the minimum wind speed for spore dispersal, WS50 (m s^{-1}) is the wind speed for the dispersal of 50% of spores, WSmax (m s^{-1}) is the wind speed for the maximum spore dispersal. The term c (unitless) is used to assign the maximum wind dispersal when WS is equal to WSmax, b (unitless) and a (m s^{-1}).

The effect of the components of partial resistance to *P. kuehnii* limits the infection and the sporulation efficiency, and the length of the latency period was simulated by coefficients modulating the efficiency of the related process, ranging from 0 (full resistance) to 1 (full susceptibility). Given the unavailability of specific data on the level of susceptibility of sugarcane varieties, in Sect. 4.5, we reported the results of a full factorial experiment where plausible ranges of partial resistance components are tested, in order to give information on model behavior. The efficiency of the infection process is then calculated by multiplying the number of infection events in a day, which refer to favorable environmental conditions triggering the disease infection, and by the wind dispersal efficiency (Eq. 8).

$$Infection\ Efficiency = Number\ of\ infection\ events * Spore\ Dispersal * HR \quad (8)$$

where HR (unitless) is the coefficient of partial host resistance. The duration of the latency period is computed as a function of air temperature, considering the minimum number of hours required at optimum temperature (Eq. 9).

$$Latency\ Completion = (LDmin) + \left(LDmin * (1 - f(T) * HR\right) \quad (9)$$

where LDmin (h) is the minimum duration of the latency period. When the latency period is completed, the host tissue becomes infectious and sporulates, producing secondary inoculum.

The last sub-model implemented in ARISE simulates the sporulation efficiency, considering hourly relative humidity and temperature as driving variables (Eq. 10).

$$Sporulation\ Efficiency = \begin{cases} f(T) * HR & if\ RH \ge RHmin \\ 0 & elsewhere \end{cases} \quad (10)$$

where RH (%) is hourly relative humidity and RHmin is minimum relative humidity for sporulation. The ARISE index (daily, unitless) is computed at the end of the daily loop (Eq. 11).

$$ARISE, d = \sum_{i=0}^{24} (Infection\ Efficiency_i * Sporulation\ Efficiency_i) \quad (11)$$

Datasets for model calibration and evaluation

ARISE was calibrated and evaluated using orange rust severity data collected during field surveys conducted in Brazil. A total of 605 field samplings were taken on 70 sugarcane farms in the Pradópolis region, state of São Paulo (21°21′34″ S, 48°03′56″, 583 a.s.l.). The climate in Pradópolis is classified as "Aw", according to the Köppen classification, corresponding to a tropical climate with summer rains, and average annual precipitation of 1401 mm and average temperature of 22 °C (Rolim and Aparecido 2015).

These data were aggregated using a basic spatial unit corresponding to the NASA-POWER grid (NASA 2018). These field samplings were conducted in plots where sugarcane varieties were considered susceptible (RB72454, SP891115, SP792233) and moderately susceptible (SP813250) to orange rust according to Chapola et al. (2016). The sugarcane phenological cycle in the area starts in February and ends in August of the following year, with the harvest period occurring between May and August. Weekly surveys were carried out, mainly during rainy periods (October to May of the second year). During each survey, two independent operators sampled five plants in different areas of the field and assigned an overall judgment of disease severity. The disease samplings were performed randomly, following a zig-zag movement and excluding the boundaries of the plot (5 m inside the plot).

The orange rust severity was estimated by considering the lower middle third of each leaf +3 according to the diagnostic scale established for brown rust (*Puccinia melanocephala*) by the Copersucar Center for Phytopathology Coordination for (Amorim et al. 1987; CDA 2010). The choice of this scale was driven by the standard method used by agronomists and technicians, given that no diagnostic scale specific for *P. kuehnii* is used yet. This assessment scale assigns disease severity based on the percentage of leaf limbus destroyed by rust and varies from 1 to 9 (Amorim et al. 1987), with 1 corresponding to the absence of the disease and 9 as total leaf destruction. In our experimental dataset, the reference data of orange rust severity used in model calibration and evaluation ranged between 1 (disease severity $\leq 0.5\%$) and 6 (disease severity $\geq 25\%$, Table S1—Supplementary Materials).

Daily meteorological data needed as input for ARISE calibration and evaluation (Brazil, period 2016–2018) and for its spatially distributed application (Brazil, India, Australia, period 1997–2017) were downloaded from the NASA-POWER database. These are maximum and minimum air temperature (°C) and relative humidity (%), average wind speed (m s^{-1}) and dew temperature (°C). Hourly weather variables were estimated from daily data: air temperature was computed according to Campbell (1985), whereas relative humidity was generated according to Bregaglio et al. (2010), based on the models proposed by Linacre (1992), Allen et al. (1998) and ASAE (1998). Hourly leaf wetness was estimated from hourly air temperature, dew point temperature, wind speed and relative humidity, according to the Classification and Regression Tree model proposed by Kim et al. (2002), considering the daily period starting at hour 0 (12 pm) and ending at hour 23 (11 pm). This choice was driven by its utmost performance in a multi-model comparison study, where six leaf wetness models were compared both in the estimation of leaf wetness and on the impact on fungal infections (Bregaglio et al. 2011). The software components EvapoTranspiration (Donatelli et al. 2006) and AirTemperature (Donatelli et al. 2010), all included in the CLIMA weather generator (Donatelli et al. 2009), were used for the generation of hourly data.

Simulation experiment design

The ARISE model was calibrated and evaluated using field observations of orange rust severity, before projecting it to assess the pathogen suitability to weather conditions in the main sugarcane-producing regions. The dataset of field observations was split into calibration and evaluation subsets by 0.5 ratio. A literature search was performed to retrieve the values of epidemiological parameters identified in laboratory or in field experiments (Table 1): the corresponding ranges were used to perform an automatic calibration of model parameters. This was conducted using a multi-start simplex algorithm, following the same procedure adopted in Bregaglio et al. (2021).

The ARISE outputs (Eq. 11) were translated into disease scores and compared with field samplings of disease severity. The simulated dynamics were analyzed using the distribution of the observed and simulated data in the 3 years of field samplings. Model performances were evaluated in three different ways, by dividing the disease data into (i) presence/absence, with absence defined as disease score = 1 and presence defined as disease scores from 2 to 6, splitting them into (ii) high/low, with low defined as disease scores 2 and 3 and high defined as disease scores from 3 to 6 (iii) using all disease scores from 1 to 6.

Model performances in reproducing observed disease data were quantified through contingency tables. In these tables, a *hit* indicates that the model correctly detects the observed data, whereas a *miss* occurs when the observation is missed by the model. A *false alarm* represents an event which is simulated but not confirmed by the observation, and a *correct negative* occurs when both the observation and the simulated output do not detect the event (AghaKouchak and Mehran 2013). The following metrics were then computed based on the contingency tables: the probability of detection (POD) (Eq. 12), which describes the fraction of the reference observations correctly identified by the simulation; the false alarm ratio (FAR) (Eq. 13), which corresponds to the fraction of events identified by the simulation but not confirmed by reference observations; the critical success index (CSI) (Eq. 14), which combines different aspects of POD and FAR and provides the overall skill of the simulation relative to observations; the bias (Eq. 15), which corresponds to the difference between the mean of the forecasts values and the mean of the observations; the accuracy (Eq. 16), which is the ratio of the correctly classified observations divided by the total number of cases; the Heidke Skill Score (HSS) (Eq. 17), which measures fractional improvements over random chance and is generally used to score multi-category events, and the Hanssen and Kuipper's Skill Score (HK) (Eq. 18), which expresses the hit rate relative to the FAR and will remain positive as long as the number of hits is greater than that of false alarms.

$$POD = \frac{hit}{hit + miss} \tag{12}$$

$$FAR = \frac{false\ alarm}{hit + false\ alarm} \tag{13}$$

$$CSI = \frac{hit}{hit + miss + false\ alarm} \tag{14}$$

$$BIAS = \frac{hit + false\ alarm}{hit + miss} \quad (15)$$

$$Accuracy = \frac{hit + correct\ negative}{total} \quad (16)$$

$$HSS = \frac{2((hit * correct\ negative) - (false\ alarm * miss))}{[(hit + miss)(miss + correct\ negative) + (hit + false\ alarm)(false + correct\ negative)]} \quad (17)$$

$$HK = \frac{(hit * correct\ negative) - (false\ alarm * miss)}{[(hit + miss)(false\ alarm + correct\ negative)]} \quad (18)$$

Environmental suitability and climatic drivers of ARISE

We performed spatially distributed simulations over large sugarcane-producing areas in Brazil, India and Australia over a 20-year period (1997–2017), to assess the environmental suitability for the pathogen and the associated variability. In order to analyze the relationships between model simulations and weather variables, contour maps of ARISE outputs were drawn in Surfer® (Golden Software, LLC) software as a function of different inputs, using the Inverse Distance Weighting (IDW) interpolation method. A graphical representation of the functions used to simulate the pathogen response to air temperature, relative humidity and wind speed is provided in the Supplementary Materials (Fig. S2). The implementation of the impact of the components of partial resistance in modulating ARISE simulations was tested by performing a full factorial experiments, where five levels of the coefficients modulating partial resistance to infection, sporulation and latency were tested, varying from 0 (complete resistant) to 1 (complete susceptible), with 0.25 interval to reproduce increasing levels of host susceptibility. Simulations were performed on a grid cell located in the São Paulo region (25°15′00.0″S 54°15′00.0″W) in 2016–2018 growing seasons. ARISE values simulated at harvest corresponding to mean and standard error in all combinations of levels of susceptibility were computed, and daily dynamic simulations were analyzed by visual representations.

Results

ARISE performances in calibration and evaluation

The model performances in calibration and evaluation datasets were positive and balanced, both considering the incidence of orange rust disease (presence/absence) and the classification of low/high disease severity. The calibrated values of ARISE parameters are reported in Table S2—Supplementary Materials.

Considering the incidence of orange rust disease, the percentage of complete matches (hit + correct negatives) was 90% (296 observations) in the calibration dataset, of which 80% were classified as hits and 10% as correct negatives. The percentage of false alarms was 9%, denoting a slight model overestimation of orange rust incidence. The percentage of misses was negligible (1%) (Fig. 2). The accuracy and POD considering disease incidence were 0.91, whereas FAR, CSI, HSS and HK resulted in 0.01, 0.90, 0.61 and 0.83, respectively (Table 2).

The ability of ARISE in reproducing high/low orange rust disease severity was lower than in reproducing its incidence. The percentage of complete matches in calibration dataset was 61%, of which 27% were hits and 34% correct negatives. The percentages of false alarms and misses were 18% and 21%, respectively. The corresponding contingency metrics computed on model outputs were POD = 0.46, FAR = 0.41, CSI = 0.35, and both HSS and HK equal to 0.17. ARISE performances in evaluation were similar than in calibration, with a higher complete percentage of matches in reproducing disease incidence than in identifying high/low orange rust severity (Fig. 2).

Considering the ability of ARISE to reproduce the different scales of orange rust severity, the percentage of complete matches between simulated and observed data was 33% (98 observations) in the calibration dataset (296). The percentage of errors equals to ±1 and ±2 on the rust severity scale was 40% and 20% (117 and 61 observations), respectively. Larger errors were significantly less frequent, with only 5% and <1% of errors equal to ±3 and ±4 degrees (Figure S1—Supplementary Materials), respectively.

Analyzing ARISE dynamics during the growing season

The daily values of simulated orange rust severity (red line, median and standard errors) in the 3 years of samplings (2016–2018) showed a good agreement with observed data (Fig. 3). The disease severity reaches the maximum value around April, and then a *plateau* was simulated from May to

Table 2 Summary statistics of the comparison between simulated and observed data of orange rust disease severity in calibration and evaluation dataset

	Calibration					
	POD	FAR	CSI	Accuracy	HSS	HK
Presence/absence of disease	0.9	0.01	0.89	0.9	0.61	0.83
High/low disease	0.55	0.41	0.4	0.61	0.21	0.21
Evaluation						
Presence/absence of disease	0.93	0.02	0.92	0.93	0.79	0.17
High/low disease	0.38	0.42	0.3	0.65	0.86	0.17

POD probability of detection, *FAR* false alarm ratio, *CSI* critical success index, *HSS* Heidke Skill Score, *HK* Hanssen & Kuipper's Skill Sc

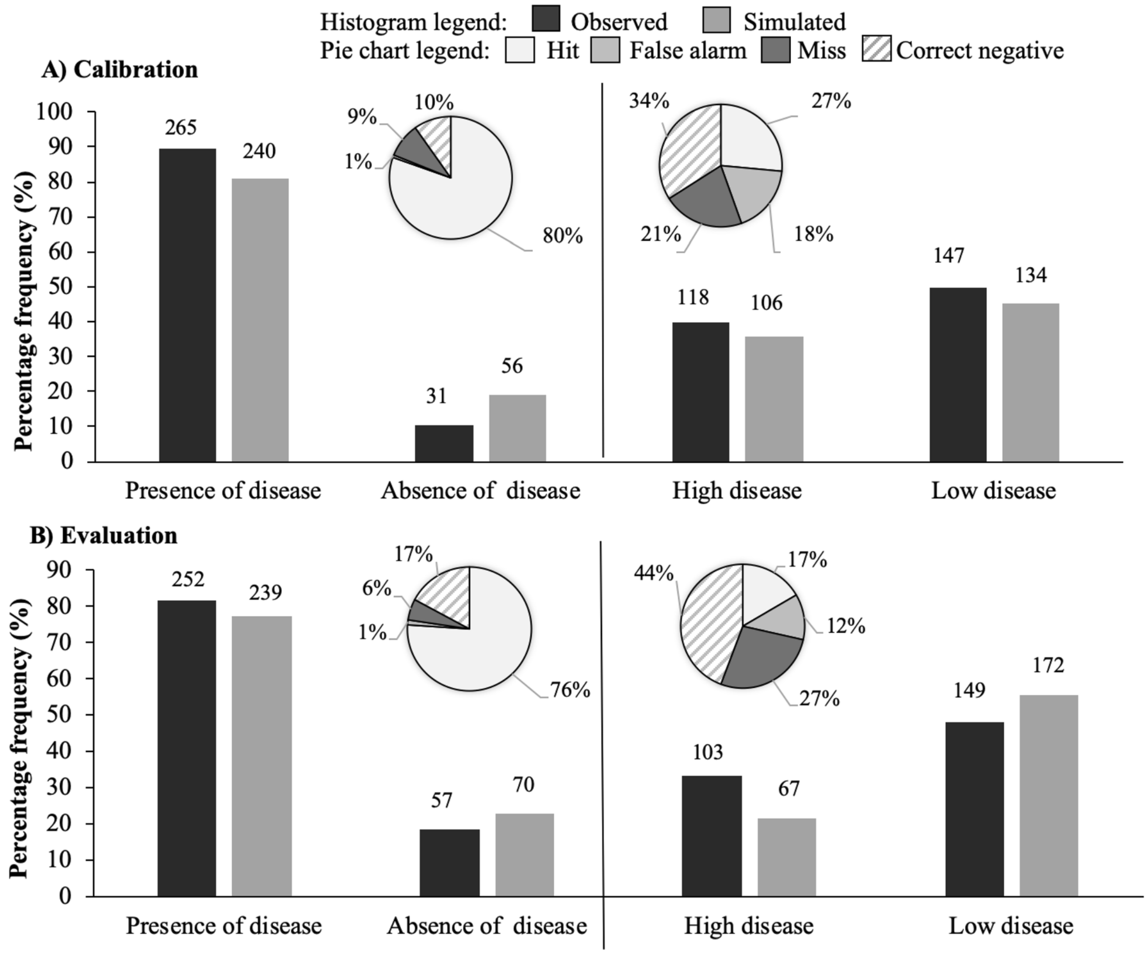

Fig. 2 Results of the comparison between simulated and observed data considering the two evaluation criteria of the presence-absence of orange rust (left figures) and low-high rust disease severity (right figures) in calibration (**A**) and evaluation (**B**) datasets. The histograms refer to the percentage frequency of observed (black) and simulated (gray) disease score, whereas pie charts report the percentages of hits, false alarms, misses and correct negatives

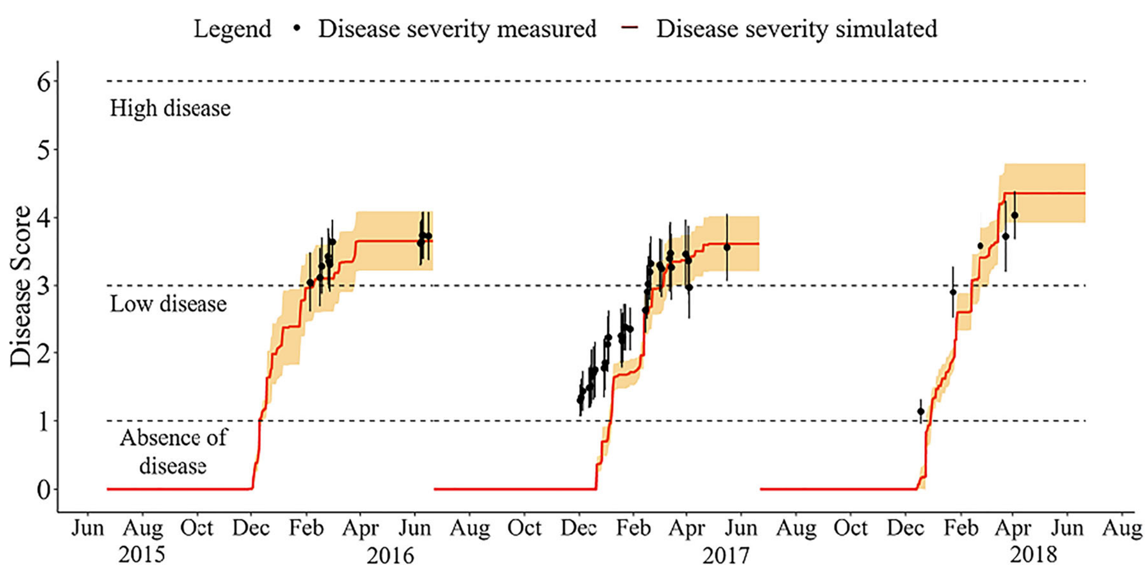

Fig. 3 Results of the comparison between simulated (solid lines) and observed disease data (circles) referred to orange rust severity in 2016–2018 growing seasons. The variability of the field surveys of the simulated (orange ribbon) and measured (error bar) data is represented by the standard error

June, due to less favorable conditions for orange rust epidemic development. ARISE model is then initialized on 21 June, and the new disease progress starts around late December–early January, depending on weather conditions. Although an underestimation can be noted in the first months of 2016, ARISE succeeded in simulating a steep increase in orange rust severity from February to April 2016, when disease observations reached the high classification (Fig. 3).

The distribution of the average observed values in the three years was not homogenous, with a higher numerosity in 2016–2017. Despite this heterogeneity, the model response was positive and presented low variability. In 2017–2018, the number of observations was the lowest, while the severity of orange rust was the highest, and the model correctly reproduced this trend.

The input weather data and the outputs of the sub-models implemented in ARISE are plotted as distributions in Fig. 4, corresponding to simulations performed in the period 1997–2017 in Pradópolis, São Paulo. The number of infection events was higher in the months with high temperature and relative humidity (October–March), whereas the latency duration was longer in the months with lower temperatures, reaching 25 days in June, July, August and September. On the contrary, the latency process approximately lasted 20 days in months characterized by high temperatures and leaf wetness duration longer than 10 h (October–May). The cumulated value of ARISE remained close to 0 until November, when it gradually increased until December, and then steeply increased from January to the end of April, reaching a *plateau* when weather conditions started to be non-conducive for the pathogen.

Analyzing the climatic drives of ARISE

The contour plots presented in Fig. 5 show the relationships between the daily rate of ARISE as a function of temperature, wind speed (Fig. 5A) and relative humidity (Fig. 5B) and using data from the spatially distributed simulations conducted in Brazil, India and Australia. It emerges that the main limiting process is sporulation (Eq. 11), which is a process limited by both thermal and moisture conditions. Sporulation

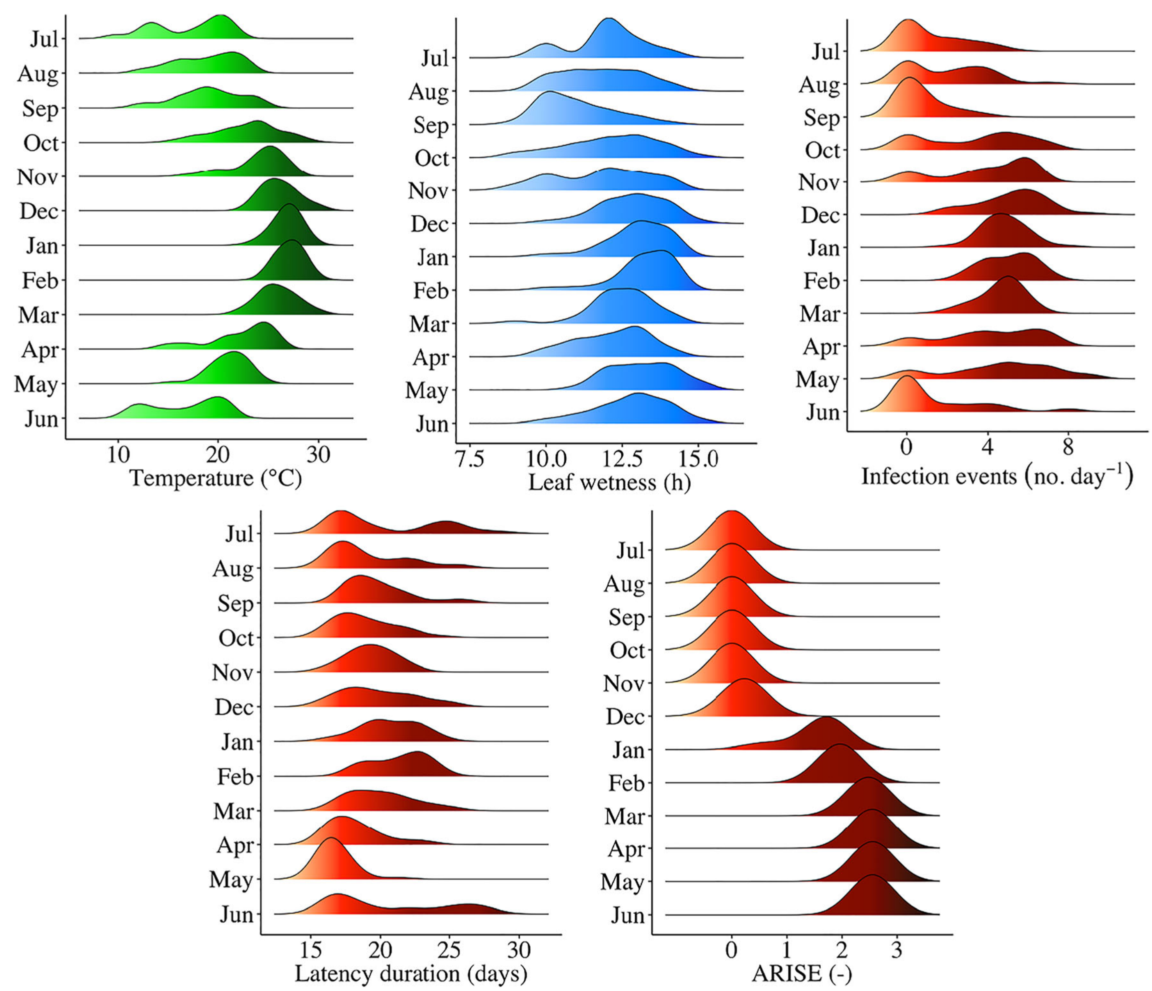

Fig. 4 Distribution curve for average values in 20 years of hourly temperature and leaf wetness, disease onset rate, number of infection events, latency duration and ARISE, results from the model, in the location (25°15′0″S, 54°15′0″W)

Fig. 5 Arise response by temperature versus relative humidity (**A**) and wind speed (**B**)

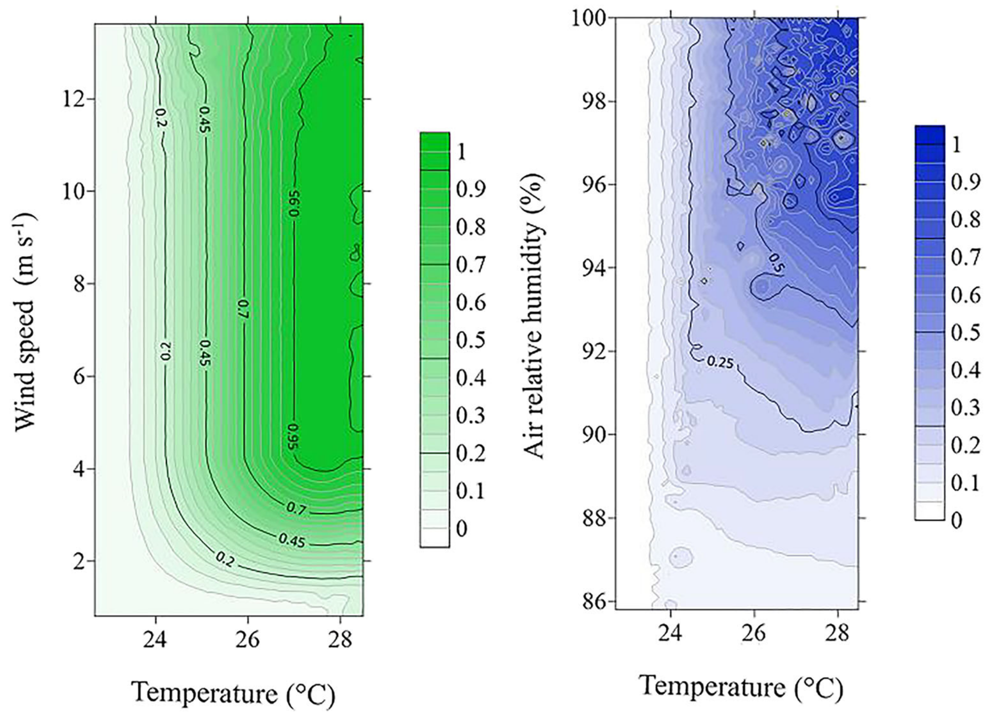

cannot occur when air relative humidity is below 80%, whereas the temperature response function of the sporulation efficiency approximates 0 around 23 °C, which is the calibrated minimum temperature for this process (Table S2—Supplementary Materials, Fig. 5B). Above this temperature threshold, ARISE simulated values increase and reach maximum values around 28 °C, in agreement with Hsieh and Fang (1981) who found that *P. kuehnii* is favored by temperatures close to 30 °C.

Concerning the relationships between wind speed and ARISE daily rate of change, there is an increasing pattern from 0.7 up to 4.2 m s^{-1}, which are the minimum and maximum calibrated values for wind dispersal, respectively. Above this value, wind speed is not a limiting factor for ARISE increase (Fig. 5A). The plots of the temperature response function to simulate infection, latency and sporulation, as well as the relative humidity response used for sporulation and the wind speed response used for spore dispersal, are reported in Figure S2—Supplementary Materials. The maximum value of the temperature function (1) was reached in correspondence of the optimum temperature calibrated for each process (22.4 °C for infection and latency, 27.6 °C for sporulation efficiency). The thermal requirements for sporulation are higher than for infection and latency, but in all processes temperatures above 30 °C are limiting. The value of the relative humidity response function is zero below the minimum threshold for sporulation, set at 80.6 %, which confirms the huge impact of moisture conditions in sporulation process. The response function of spore dispersal driven by wind speed starts to increase when daily wind speed is above the minimum threshold for spore dispersal (0.7 m s^{-1}) and increases up to 1 when wind speed is above 4.2 m s^{-1}.

Spatial application of ARISE in Brazil, India and Australia

The results of the spatially distributed application of ARISE in the main sugarcane areas of Brazil, India and Australia are shown in Fig. 6, where also average air relative humidity and air temperature are plotted, considering a 20-year period (1997–2017). Our results indicate that India was the most favorable areas for orange rust epidemics, mainly because of its more suitable thermal conditions. The calibrated optimal temperature for the development of orange rust was 22.4 °C, with a maximum of 29 °C: in India, the mean value of temperature fell in this range in almost all the cell grids. It is worth noting that only in a small part of the southwest region, ARISE values were below 0.5. In the Southern Brazilian areas, the mean temperature fluctuated around 14 °C, leading to low ARISE values (<0.5), despite the high relative humidity. In Australia, ARISE outputs followed the gradient of relative humidity, with higher values (≈2.0), moving from central to coastal areas. Despite the variability of model results, ARISE values were consistent and comparable across sugarcane growing areas, ranging from 0 to around 2.

A spatial analysis of model outputs in a 10-day period and annual (20 years) scale can be found in the Supplementary Materials in the form of animated gif files. Analyzing the temporal distribution of the 10-day scale, ARISE started to increase in November in the Brazilian northeastern region.

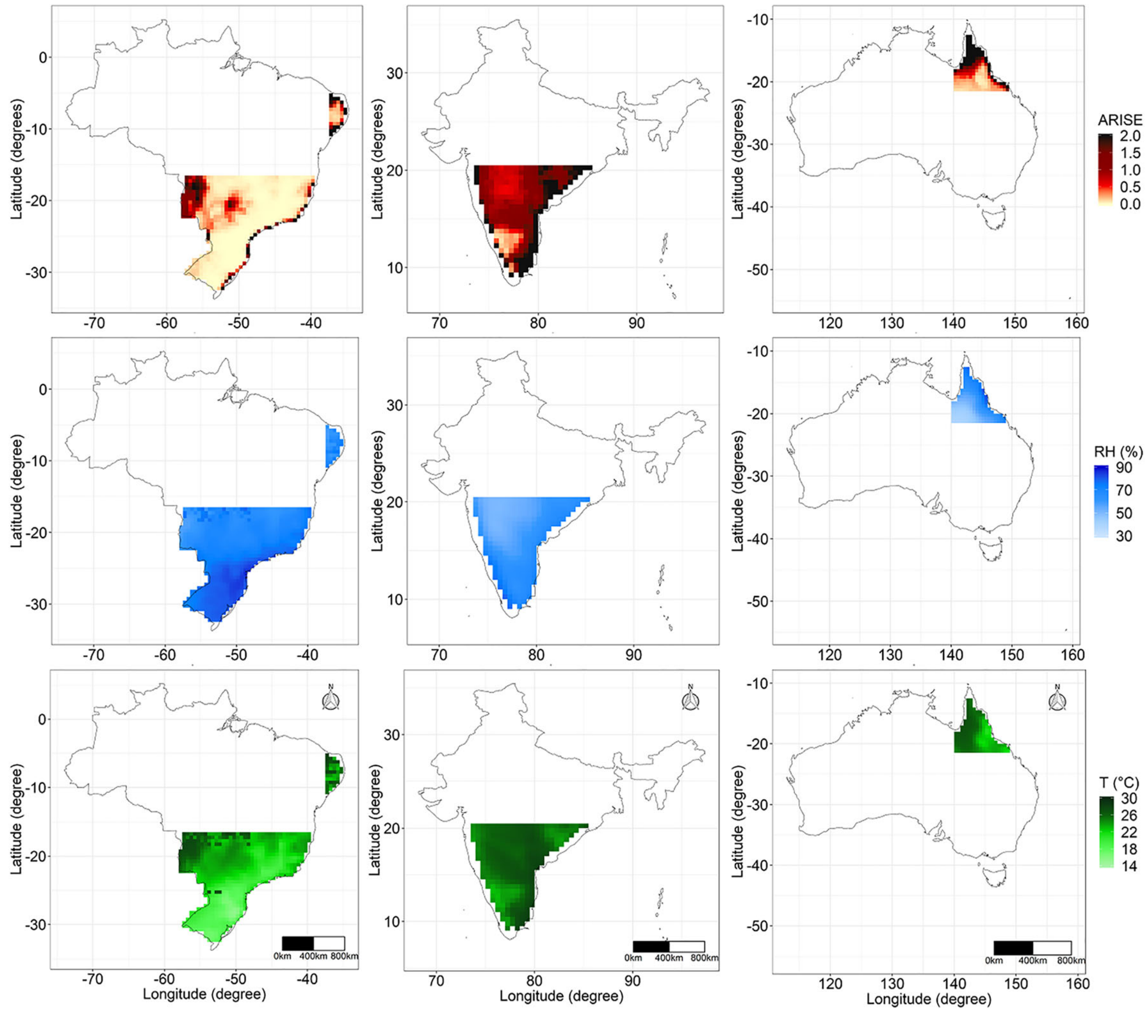

Fig. 6 Spatialization of the average ARISE outputs at the end of summer (**A**—Brazil; **B**—India; **C**—Australia), relative humidity (RH, %), (**D**—Brazil; **E**—India; **F**—Australia) and temperature (T, °C), (**G**—Brazil; **H**—India; **I**—Australia) from 1997 to 2017

Then, in December, ARISE increased in the center-west region and in the region of São Paulo, which is the main Brazilian sugarcane production area. In India, positive values occurred in the first month of simulation (July). Similarly to the simulations performed in Brazil, in India simulated disease severity started to increase in the coastal region and then spread towards the interior regions, constantly reaching high values. Model results in Australia were similar than in Brazil, with ARISE outputs starting to grow in September in the coastal areas, whereas Indian sugarcane regions were associated to higher ARISE values. In the annual scale animation (1997–2017), we observed an agreement of the simulations over the same regions and over of the different years, despite a large inter-annual variability in absolute values.

ARISE simulated with partial resistance component

The sensitivity of the model outputs as modulated by the components of partial resistance to infection, sporulation and latency is shown in Fig. 7, where ARISE was run on a grid cell sampled in the São Paulo region (25°15′00.0″S 54°15′00.0″W) in 2016–2018 growing seasons. Here, five values of the coefficients are tested, from 0 (complete resistant) to 1 (complete susceptible), with 0.25 interval to represent increasing levels of host susceptibility. The simulated cumulated value of the efficiency of infection (Fig. 7A) and sporulation (Fig. 7C) showed an increasing gradient from 0 in the simulations with complete resistance to the maximum value in the simulation with full host susceptibility. The simulations performed with the highest resistance to the latency duration (Fig. 7B) resulted in doubling the minimum duration of the latency period (Eq. 9, 30 days), with lower resistance shortening the length of the period, with the variability due to air temperature. The simulations performed setting all host resistance coefficients at 0, corresponding to a full resistant variety, resulted in no disease severity (Fig. 7D). The simulations performed with increasing levels of host susceptibility led to average ARISE values of 0.0672 (se = 0.0014) for moderately resistant (HR

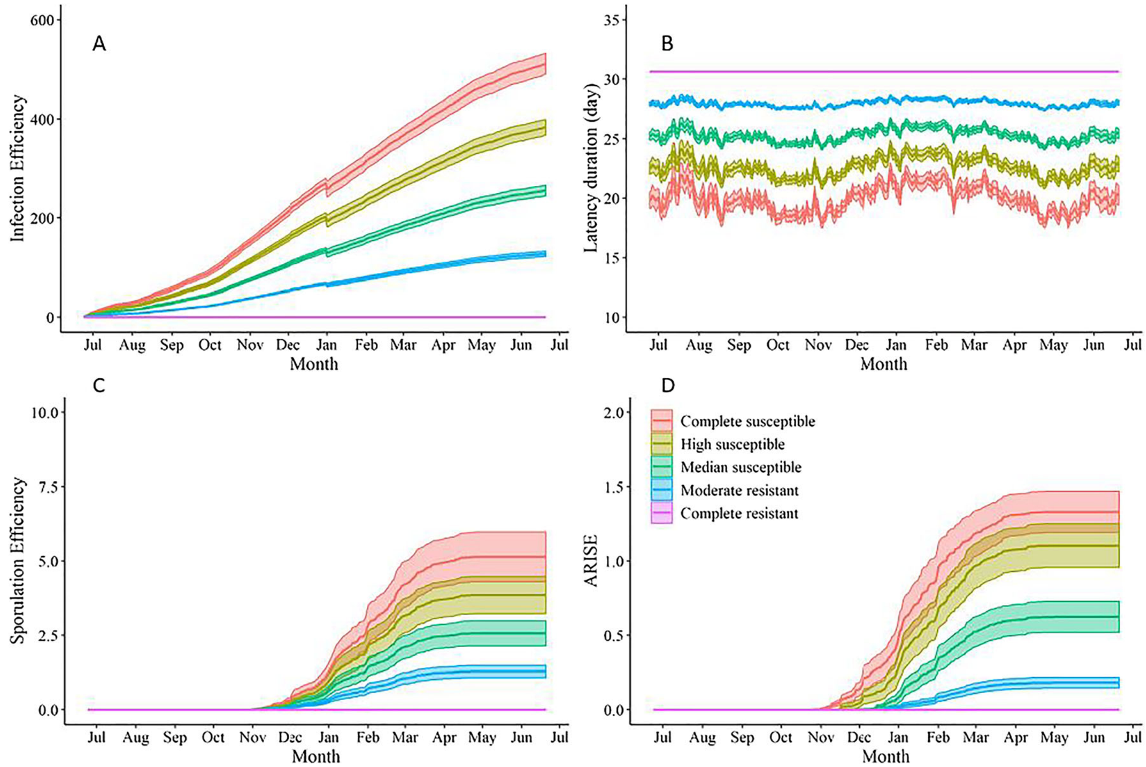

Fig. 7 Results from the full factorial experiment testing different levels of partial resistance, simulated in Pradopolis (25°15′00.0″S 54°15′00.0″W). **A**) Simulated infection efficiency (number of infection events); **B**) simulated latency duration in days; **C**) simulated sporulation efficiency; **D**) simulated ARISE values. The tested values of the partial host resistance coefficients corresponded to full resistance (0), moderate resistance (0.25), median susceptibility (0.50), high susceptibility (0.75) and full susceptibility (1). The average dynamic data are plotted as solid lines, and the shaded areas correspond to average values ± one standard error

coefficients = 0.25), 0.2405 (se = 0.0045) for median susceptible (HR coefficients = 0.5), 0.4519 (se = 0.0074) for high susceptible (HR coefficients = 0.75) and 0.5780 (se = 0.0085) for complete susceptible (HR coefficients = 1).

Discussion

The ARISE process-based model presented here simulates the suitability of weather conditions for sugarcane orange rust disease, focusing on key processes underlying the epidemiologic cycle of *P. kuehnii*, i.e. infection, spore dispersal, latency duration and sporulation efficiency. Specific information about the life cycle of *P. kuehnii* has not been extensively found in the literature; therefore, we complemented available information with experimental data referred to another species of the same genus, *Puccinia melanocephala,* which also causes serious yield losses in sugarcane. We assembled generic process-based sub-models for each phase of the epidemiologic cycle, and we adapted them to simulate *P. kuehnii* thermal and moisture requirements through parameterization, based on biologic ranges retrieved from published data.

The optimum, maximum and minimum temperature for infection and latency were set to 22 °C, 30 °C and 10 °C, respectively. This agrees with the values obtained in laboratory experiments performed by Magarey et al. (2004), Martins (2010) and Minchio et al. (2017), who found a range of temperatures between 10 and 30 °C, with optimal values close to 22 °C. Our calibration found a minimum and optimum temperature for sporulation equal to 22 °C and 27 °C, similar to Hsieh and Fang (1981), who measured 22 °C and 30 °C, respectively. This results also agree with Chaulagain et al. (2020), who developed a weather-based predictive modeling of orange rust of sugarcane in Florida, finding a positive and highest correlation between orange rust severity and hours with average temperature between 20 °C and 22 °C during the night period and a negative correlation for number of hours with maximum temperature greater than 32 °C, in line with the maximum temperature calibrated here.

The calibrated moisture requirements were 80.6% as minimum relative humidity for sporulation and 7 h of leaf wetness for the infection process, in agreement with Magarey et al. (2004). The minimum wetness duration requirement is close to the values reported by Martins (2010). This result agrees with Sentelhas et al. (2016), who founded that the orange rust outbreaks were associated with a very humid environment. The optimal duration of the latency period was set at 15 days, 1 day shorter than in Martins (2010). The disease progress curve started to increase in November, reaching the highest values from January until the end of April, in agreement with Chapola et al. (2016) and Araújo et al. (2013). These authors reported an increase in the disease severity at the end of November, with peaks between February and April, when moisture is high and air temperature is warm, which are favorable conditions for orange rust development (Magarey et al. 2004). After this peak, ARISE reached a *plateau* from May until June, when the model is reinitialized, to simulate the main harvest period. This establishment of the index occurs in consequence of not suitable weather conditions for the pathogen.

ARISE detected with accuracy and precision, based on contingency table metrics, the presence and absence of the disease, although it was less capable of differentiating low and high disease severity levels. This outcome is relevant for decision makers at different levels, from sugarcane growers who need to optimize the scheduling of chemical treatments, and can use ARISE with forecasted weather data to prevent the occurrence of secondary infections, as well as for players from the private sector who can drive their investments in new plantations based on the suitability of weather conditions to the orange rust pathogen. According to Chaulagain et al. (2019), in an experiment performed in Florida testing the application timing of fungicides for the management of sugarcane orange rust, the preventive applications at the beginning of epidemics led to the best control strategy during the season. In the same work, the applications at mid or late epidemic stages were still useful, to a lower degree, for the partial control of orange rust.

Once the model was calibrated in Brazil with an extended dataset of field observations, we applied ARISE over three world's main sugarcane producers—Brazil, India and Australia (FAO 2019). This application should be considered as a proof of concept of the capability of ARISE to be applied across environments while evaluating the associated variability in simulated disease severity, rather than a definitive assessment of weather suitability to the pathogen in these areas. Our aim here was to develop a process-based simulation model which reproduces the epidemiology of orange rust pathogen. We found that, even without a specific calibration, which could not be done due to lack of experimental data, the range of variability in ARISE outputs in India and Australia was comparable to the one simulated in the area where the model was calibrated (Brazil). Given that the processes embedded in ARISE refer to epidemiological processes which are driven by the pathogen's hydro-thermal requirements, the model application in other sugarcane growing areas represent a valuable indication of its adequacy, besides a refinement of calibration could be needed when new field data will become available in dedicated experimental trials.

Since the population genetics and the evolutionary potential of this pathogen is not yet well understood, evaluating its weather suitability based on current knowledge is the first step towards forecasting the pathogen suitability to across geographical and climatic conditions, also in light of the undergoing climatic changes (Bisonard et al. 2020). ARISE simulations confirmed that environmental conditions mostly favoring the disease are high relative humidity and temperature (Minchio et al. 2017). Spatial simulations performed in India led to the highest suitability to orange rust due to the thermal conditions, which were favorable on most areas except in regions where temperature was below 22 °C. These results agree with Sanjel et al. (2019), which reported that temperatures between 20 and 22.2 °C were conducive to appearance of severe disease symptoms in the field. High moisture conditions determined an early start of the disease in all simulated regions, as ARISE started to increase in coastal areas where relative humidity was higher. Our results are in agreement with Sentelhas et al. (2016), who analyzed the agro-climatic suitability for sugarcane orange rust, confirming that Queensland regions close to the Pacific Coast were more suitable to the orange rust pathogen. Also, the temporal dynamic of disease severity simulated in our study complies with Sentelhas et al. (2016), because early symptoms started to be simulated in September in Australia and in November in Brazilian northeast region, whereas ARISE started to increase in December in the center-east of São Paulo, as also reported by Araújo et al. (2013).

The information on the level of susceptibility to orange rust of current sugarcane varieties is scarce in literature (Klosowski et al. 2013a). Few studies were performed in Brazil (Araújo et al. 2013; Klosowski et al. 2015; Chapola et al. 2016). According to Klosowski et al. (2013a), orange rust represents a major concern in breeding programs of sugarcane, since genotypes that are used as parent in crosses to generate new cultivars are generally susceptible to the pathogen. The full factorial experiment presented here is meant to release information on model behavior, rather than being aimed at reproducing the levels of susceptibility of specific varieties. We explored all plausible values of partial resistance components, giving a complete overview of their impact on ARISE simulation, making the model ready to be applied on real varieties, once information on their susceptibility to orange rust pathogen are made available. The results of our simulation experiment suggest that disease severity strongly varies across levels of host resistance and that our model provides a mean to reproduce the partial components of host resistance which is controlled by one major gene and several genes acting quantitatively (Klosowski et al. 2013a).

We acknowledge the possible limitation due to the use of gridded weather data at a coarse spatial resolution as input to ARISE, even if this scale can be considered adequate for real-time monitoring over large areas. An ideal dataset for ARISE application at field level would comprise in situ ground weather stations placed in close proximity to the sugarcane fields, but these were not available in the study area (Pereira et al. 2002). However, the key outcome of our study is the development of a process-based model capable to simulate the epidemiology of orange rust pathogen with parameters with biological meaning. ARISE can be easily interfaced with different data sources as input, ranging from IoT sensors to public databases, as is the case presented in this study. Moreover, Valeriano et al. (2019) compared the same source of gridded weather data with ground weather stations in an area close to the one targeted by ARISE calibration, finding very good similarity especially for temperature data.

The use of the NASA-Power database, where daily weather data are available, required the development of a modeling layer on the bottom, in order to generate hourly inputs for ARISE. Besides the selection of the modeling approaches to downscale daily data at hourly resolution has been driven by their good performances in previous studies, the generation of hourly inputs could be performed with alternative approaches in future studies, or even avoided when hourly data will be available from ground weather stations.

ARISE performance in reproducing disease incidence was higher than in simulating disease severity. However, the model accuracy in differentiating low and high disease severity levels was still acceptable: in Figure S1—Supplementary Materials, we showed that model errors are mostly comprised within ±1 and ±2° of the severity scale (40% and 20% respectively), whereas larger model errors occurred only in 6% of the cases. These results strengthen the model accuracy, especially given the uncertainty associated with visual observations of orange rust severity, which are affected by an inner subjectivity. Our rationale was to develop a model where all key epidemiological processes are formalized and driven by parameters which were calibrated within their biological ranges, according to state-of-the-art knowledge from literature. Their adequateness in reproducing specific components of the pathogen's cycle could only be tested when reference data specific for each process have been measured, e.g. by means of spore traps for evaluating the intensity of sporulation, or laboratory analysis on sugarcane leaves to determine infection events. Given that the ranges of the parameters driving the epidemiological processes were retrieved from published studies performed in laboratory, i.e. ideal conditions, they could not be fully representative of the huge variability in pathogen populations present in the sugarcane fields. However, when new data become available, the model can easily be re-calibrated with new information and data. This will minimize the risk of including additional sources of uncertainty in the values of the parameters, while contributing to improve its performances.

The uncertainty related to the assessment of the observed disease data and the disease assessment scale is a criticality of our study. The relatively low number of observations with high scores could have biased model performances, leading to lower accuracy in the reproduction of high and low disease levels. Although disease scales specific for orange rust severity are available, as the one developed by Klosowski et al. (2013b), our observations were carried out using the scale recommended in São Paulo area for brown rust (*Puccinia melanocephala*), i.e. the one operationally used by field technicians to evaluate orange rust symptoms. This decision was driven by the availability of an extended dataset of field observations, compliant with the current sampling methodology adopted in the sugarcane mills.

Besides these criticalities, it should be noted that ARISE succeeded in reproducing observed dynamics of orange rust severity and in simulating comparable values across sugarcane growing areas, coherently with the variability of weather conditions explored. Also, ARISE has been applied so far to one specific fungal disease, but the generic methodological background of the sub-models of the different epidemiologic phases can be easily reused or extended to foster the simulation of other fungal pathogens. In addition, the results of the spatial model application provide a quantitative risk assessment of sugarcane orange rust epidemics, which can be used, e.g. by stakeholders in the sugarcane sector in order to avoid planting susceptible varieties in those regions where a high level of ARISE was simulated, as well as offer the potential of developing real-time decision support to the timely application of fungicides according to weather conduciveness for pathogen infection (Sentelhas et al. 2016; Chaulagain et al. 2020).

Conclusion

Developing process-based models to predict the occurrence and the dynamic of plant diseases is a hot topic in the modeling community. This is especially valid in situations where the disease is relatively new and no decision support system is available yet, as is the case of orange rust on sugarcane in Brazil. The ARISE model aims at filling this gap, by coupling models reproducing the key epidemiological processes life cycle of the pathogen, which have been parameterized using literature information. Despite the need of additional datasets to further prove its reliability, the ARISE application in calibration/evaluation over main sugarcane-producing countries demonstrated its potential to be used for in-season disease forecasting, as well as to evaluate the inter-annual variability of disease pressure in alternative climatic and/or management scenario analyses.

Supplementary Information The online version contains supplementary material available at https://doi.org/10.1007/s00484-021-02162-5.

Availability of data and materials The data that support the findings of this study are available on request from the corresponding author, Valeriano, TTB.

Code availability The model source code is available on request from the corresponding author, Valeriano, TTB.

Funding This research was supported by the Coordenacao de Aperfeicoamento de Pessoal de Nivel Superior—Brasil (CAPES)—Finance code 001 and by the Conselho Nacional de Desenvolvimento Cientifico e Tecnologico—Brasil (CNPQ)—Finance code 141291/2017-6. This research was also supported by the AgriDigit-Agromodelli project (DM n. 36502 of 20/12/2018), funded by the Italian Ministry of Agricultural, Food and Forestry Policies and Tourism and by MatHiLDE (Modelling pests and diseases impact on hazelnut production) project, funded by Luxembourg National Research Fund—Industrial Fellowships (2019-1 call).

Declarations

Conflict of interest The authors declare no competing interests.

References

AghaKouchak A, Mehran A (2013) Extended contingency table: performance metrics for satellite observations and climate model simulations. Water Resour Res 49:7144–7149

Allen RG, Pereira LS, Raes D, Smith M (1998) Crop evapotranspiration: guidelines for computing crop water requirements. UN-FAO, Rome, Italy

Amorim L, Bergamin Filho A, Sanguino A, Ardoso COM, Moraes VA, Fernandes CR (1987) Evaluation methodology of sugarcane rust (Puccinia melanocephala). Techn Bull Copersucar: São Paulo 39: 13–16

Araújo KL, Canteri MG, Gilio TAS, Neubauer RA, Sanches PB, Sumida CH, Giglioti EA (2013) Genotypic resistance and monitoring of favourability for the occurrence of orange rust in sugarcane. Summa Phytopathol 39(4):271–275

ASAE Standards (1998) EP406.2: heating, cooling, and ventilating greenhouses. St. Joseph, MI, USA

Aylor DE (1982) Modelling spore dispersal in a barley crop. Agric Meteorol 26:215–219

Barbasso D, Jordão H, Maccheroni W, Boldini J, Bressiani J, Sanguino A (2010) First report of Puccinia kuenhii, causal agent of orange rust of sugarcane, in Brazil. Plant Dis 94:1170

Basso B, Cammarano D, Carfagna E (2013) Review of crop yield forecasting methods and early warning systems. In: Proceedings of the First Meeting of the Scientific Advisory Committee of the Global Strategy to Improve Agricultural and Rural Statistics. FAO Headquarters, Rome, pp 18–19

Bisonard EM, Hamada E, Angelotti F, Gonçalves RRV, Rago AM (2020) Evolution of peanut black spot in the main producing areas of Argentina and Brazil under climate change. Rev Bras Geog Fís 13:1778–1791

Bordonal RO, Carvalho JLN, Lal R, Figueiredo EB, Oliveira BG, La Scala JN (2018) Sustainability of sugarcane production in Brazil. A review. Agron Sustain Dev 38(13). https://doi.org/10.1007/s13593-018-0490-x

Bregaglio S, Donatelli M (2015) A set of software components for the simulation of plant airbone diseases. Environ Model Softw:1–9

Bregaglio S, Donatelli M, Confalonieri R, Acutis M, Orlandini S (2010) An integrated evaluation of thirteen modelling solutions for the generation of hourly values of air relative humidity. Theor Appl Climatol 102:429–438. https://doi.org/10.1007/s00704-010-0274-y

Bregaglio S, Donatelli M, Confalonieri R, Acutis M, Orlandini S (2011) Multi metric evaluation of leaf wetness models for large-area application of plant disease models. Agric For Meteorol 151:1163–1172

Bregaglio S, Cappelli G, Donatelli M (2012) Evaluating the suitability of a generic fungal infection model for pest risk assessment studies. Ecol Model 247:58–63

Bregaglio S, Fischer K, Ginaldi F, Valeriano T, Giustarini L (2021) The HADES yield prediction system—a case study on the Turkish hazelnut sector. Front Plant Sci 12. https://doi.org/10.3389/fpls.2021.665471

Campbell GS (1985) Soil physics with BASIC: transport models for soil–plant systems. Elsevier, Amsterdam

CDA (2010) Agricultural Defense Coordination. In: Orange sugar cane rust. Technical Information, São Paulo

Chapola RG, Hoffmann HP, Massola NS Jr (2016) Reaction of sugarcane varieties to orange rust (Puccinia kuehnii) and methods for rapid identification of resistant genotypes. Trop Plant Pathol:41–139

Chaulagain B, Raid RN, Dufault N, Van Santen E, Rott P (2019) Application timing of fungicides for the management of sugarcane orange rust. Crop Prot 119:141–146

Chaulagain B, Small I, Shine JM, Fraisse C, Raid RN, Rott PCE (2020) Weather-based predictive modelling of orange rust of sugarcane in Florida. Phytopathology 110(3):626–632

Chaves A, Simões Neto DE, Dutra Filho JA, Oliveira AC, Rodrigues WDL, Pedrosa EMR, Borges VJL, França PRP (2013) Presence of orange rust on sugarcane in the state of Pernambuco, Brazil. Trop Plant Pathol 38(5):443–446

CONAB—Companhia Nacional de Abastecimento (2019) Agricultural observatory: monitoring the Brazilian crop (sugarcane) third survey (Safra 2018/2019) 5(3)

Donatelli M, Bellocchi G, Carlini L (2006) Sharing knowledge via software components: models on reference evapotranspiration. Eur J Agron 24:1186–1192

Donatelli M, Bellocchi G, Habyarimana E, Bregaglio S, Confalonieri R, Baruth B (2009) CLIMA, a modular weather generator. In: Anderssen RS, Braddock RD, Newham LTH (eds) 18th World IMACS Congress and MODSIM09 International Congress on Modelling and Simulation. Modelling and Simulation Society of Australia and New Zealand and International Association for Mathematics and Computers in Simulation. July 2009, pp 852–858. ISBN: 978-0-9758400-7-8. http://www.mssanz.org.au/modsim09/C3/donatelli_C3a.pdf

Donatelli M, Bellocchi G, Habyarimana E, Bregaglio S, Baruth B (2010) AirTemperature: extensible software library to generate air temperature data. SRX Computer Science (in press)

(FAO) Food and Agriculture Organization of the United Nations (2019) FAOSTAT Database. http://www.fao.org/faostat/en/#home. Accessed 02 April 2021

Ferrari JT, Harakava R, Domingues RJ, Terçariol IML, Töfoli JG (2013) Orange rust of sugarcane in Brazil. Biológico 75(1):71–74

Gillespie TJ, Sentelhas PC (2008) Agrometeorology and plant disease management—a happy marriage. Sci Agric 65:71–75

Hawksworth DL, Kirk PM, Sutton BC, Pegler DN (1995) Ainsworth & Bisby's dictionary of the fungi. CAB international, Wallingford

Hsieh WH, Fang JB (1981) Studies on sugarcane rust disease. 1980-81 Annu Rep Taiwan Sugar Res Inst:22–23

Hsieh WH, Lee CS, Chan SI (1977) Rust disease of sugarcane in Taiwan: the causal organism Puccinia melanocephala Sydow. Taiwan Sugar 24(5):416–410

Infante D, Martinez B, Gonzalez E, Gonzalez N (2009) Puccinia kuehnii (Kruger) Butler y Puccinia melanocephala H. Sydow y P. Sydow en el cultivo de la caña de azúcar. Rev Protección Vegetal 24:22–28

Kim KS, Taylor SE, Gleason MML, Koehler KJ (2002) Model to enhance site-specific estimation of leaf wetness duration. Plant Dis 86:179–185

Klosowski AC, Bespalhok Filho JC, Ruaro L, May De Mio LL (2013a) Inheritance of resistance to orange rust (Puccinia kuehnii) in sugarcane families from crosses between parents with different orange rust reactions. Sugar Tech:1–5

Klosowski AC, Ruaro L, Bespalhok Filho JC, May De Mio LL (2013b) Proposal and validation of diagrammatic scale for assessment of orange rust of sugarcane. Trop Plant Pathol 38(2):166–171

Klosowski AC, Bespalhok Filho JC, Ruaro L, May De Mio LL (2015) Reaction of commercial cultivars and assessment date of orange rust sugarcane. Biosci J 31(2):489–498

Lima LL, Scaloppi EAG, Barreto LF, Barreto M (2017) Temperatures and leaf wetness duration on orange rust development in sugarcane (Puccinia kuehnii). Summa Phytopathol 43(2):132–135

Linacre E (1992) Climate data and resources: a reference and guide. Routledge, London

Magarey RC (2000) Orange rust. In: Rott P, Bailey RA, Comstock JC, Croft BJ, Girad J-C, Saumtally S (eds) A guide to sugarcane diseases. CIRAD—ISSCT, Montpellier, pp 121–125

Magarey RC, Croft BJ, Willcox TG (2001) An epidemic of orange rust on sugarcane in Australia. Proc Int Soc Sugar Cane Technol 23:410–416

Magarey RC, Neilsen WA, Magnanini AJ (2004) Environmental requirements for spore germination in the three sugarcane leaf pathogens. In: Conference of the Australasian Society of Sugar Cane Technologists held at Brisbane, Queensland, pp 1–7

Magarey RD, Sutton TB, Thayer CL (2005) A simple generic infection model for foliar fungal plant pathogens. Phytopathology 95:92–100

Mallaiah KS, Rao AS (1982) Aerial dissemination of groundnut rust uredinospores. Trans Br Mycol Soc 82:21–28

Manici LM, Bregaglio S, Fumagalli D, Doxnatelli M (2014) Modelling soil borne fungal pathogens of arable crops under climate change. Int J Biometeorol:1–13

Martins TD (2010) Epidemiological aspect of sugarcane orange rust. Thesis (PhD in Phytopathology) Escola Superior de Agricultura " Luiz de Queiroz", Universidade de São Paulo, Piracicaba, 2010

Minchio CA, Canteri MG, Rocha JA (2011) Germination of uredospores of Puccinia kuehnii subjected to different temperatures and incubation times. Summa Phytopathol 34:211–214

Minchio CA, Fantin LH, Oliveira KB, Rocha JA, Canteri M (2017) Morphological changes of the Urediniospore of Puccinia kuehnii germ tube in function of temperature. Agron Sci Biotechnol 3:19–24

Mistura TF (2016) Factors affecting success and longevity of resistant varieties to control sugarcane rusts. (Master dissertation), Federal University of São Carlos

Moreira AS, Nogueira Junior AF, Gonçalves CRNB, Souza NA, Bergamin Filho A (2018) Pathogenic and molecular comparison of Puccinia kuehnii isolates and reactions of sugarcane varieties to Orange rust. Plant Pathol 67(8):1687–1696

NASA (2018) NASA surface meteorology and solar energy: methodology. NASA. https://power.larc.nasa.gov/documents/POWER_Data_v9_methodology. Accessed 8 April 2018

Pereira AR, Angelocci LR, Sentelhas PC (2002) Agrometeorologia: fundamentos e aplicações práticas. Agropecuária, Guaíba, 478p

Rolim GS, Aparecido LEO (2015) Camargo, Köppen and Thornthwaite climate classification systems in defining climatical regions of the state of São Paulo, Brazil. Int J Climatol 36:636–643

Rott PC, Kaye C, Naranjo MM, Shine J Jr, Sood S, Comstock JC, Raid RN (2016) Controlling sugarcane diseases in Florida: a challenge in constant evolution. Proc Int Soc Sugar Cane Technol 29:595–600

Sanjel S, Hincapie M, Sood S, Comstock JC, Raid RN, Rott P (2016) Evidence for variation in virulence of the sugarcane orange rust pathogen in Florida. 46th American Society of Sugar Cane Technologists Annual Meeting, 13–15 June 2016, St Pete Beach, FL. Sugar Journal 79(1):29–30

Sanjel S, Chaulagain B, Small I, Comstock JC, Hincapie MA, Raid R, Rott PC (2019) Comparison of progress of brown rust and orange rust and conditions conducive for severe epidemic development during the sugarcane crop season in Florida. Plant Dis 103:825–833

Sentelhas PC, Santos DL, Monteiro LA, Soares-Colletti AR, Pallone Filho WJ, Donzelli JL, Arrigoni EB (2016) Agro-climatic favorability zones for sugarcane orange rust as a tool for cultivar choice and disease management. Crop Prot 84:88–97

Valeriano TTB, Rolim GS, Bispo RC, Moraes JRSC, Aparecido LEO (2019) Evaluation of air temperature and rainfall from ECMWF and NASA gridded data for southeastern Brazil. Theor Appl Climatol 137:1925–1938

Vaseduva RS (1958) Report of the division of mycology and pathology. Sci. Rep. agric. Res. Inst. N. Delhi. Rev Appl Mycol 1956-1957:86–100

Yan W, Hunt LA (1999) An equation for modelling the temperature response of plants using only the cardinal temperatures. Ann Bot 84:607–614

Zhao D, Glynn NC, Glaz B, Comstock JC, Sood S (2011) Orange rust effects on leaf photosynthesis and related characters of sugarcane. Plant Dis 95:640–647